Weak localization of magnons in chiral magnets

Martin Evers, Cord A. Müller, and Ulrich Nowak

Fachbereich Physik, Universität Konstanz, 78457 Konstanz, Germany

We report on the impact of the Dzyaloshinskii-Moriya interaction on the coherent backscattering of spin waves in a disordered magnetic material. This interaction breaks the inversion symmetry of the spin-wave dispersion relation, such that $\omega_{\mathbf{k}} = \omega_{2\mathbf{K}^{\mathrm{I}}-\mathbf{k}} \neq \omega_{-\mathbf{k}}$, where $\mathbf{K}^{\mathrm{I}}$ is related to the Dzyaloshinskii-Moriya vectors. The nonequivalence of $\mathbf{k}$ and $-\mathbf{k}$ also means that time-reversal symmetry is broken. As a result of numerical investigations we find that the backscattering peak of a wave packet with initial wave vector $\mathbf{k}_0$ shifts from $-\mathbf{k}_0$ to $2\mathbf{K}^{\mathrm{I}} - \mathbf{k}_0$, such that the backscattering wave vector and the initial wave vector are in general no longer antiparallel. The shifted coherence condition is explained by a diagrammatic approach and opens up an avenue to measure sign and magnitude of the Dzyaloshinskii-Moriya interaction in weakly disordered chiral magnets. Surprisingly, although time-reversal symmetry is broken, our system shows coherent backscattering as a manifestation of weak localization, which is due to the fact that reciprocity is still preserved.

I. INTRODUCTION

Spin waves or magnons, low-energy excitations of the magnetic ground state of a solid, have been studied extensively since their first proposal [1,2]. In recent years, they have drawn much attention in connection with new effects such as the spin Seebeck effect [3], room-temperature Bose-Einstein condensation [4], magnonic supercurrents [5], or magnonic topological insulators [6]. Furthermore, magnonic transport is a promising candidate for future data-processing devices [7], because—in contrast to conventional electronic- or spintronic-based technology—magnons do not suffer from Joule heating [8].

Interesting properties arise in chiral magnets, where the antisymmetric exchange interaction—the Dzyaloshinskii-Moriya (DM) interaction [9,10]—induces, for example, non-collinear ground states [11], skyrmions [12], Berry phase materials [6], and a noninversion symmetric dispersion of the magnons [13–15]. The DM interaction originates from spin-orbit interactions and is, hence, naturally linked to the upcoming field of spin orbitronics [16–21]. In this context it is important to examine the role of defects, because, on the one hand, real magnetic materials inevitably contain some amount of disorder whose impact on device functionality needs to be evaluated. On the other hand, disorder also entails unique effects of its own that may be harnessed for specific applications.

Most prominent in this context is Anderson localization [22] in strongly disordered materials, where coherent transport of waves comes to a complete stop. But already moderately disordered materials can show interesting weak-localization phenomena, for example, the well-known coherent backscattering (CBS) effect [23]. When a monochromatic wave is launched with wave vector $\mathbf{k}_0$ into the disordered system, CBS can be observed as an enhanced average intensity above the incoherent background, usually around the wave vector $-\mathbf{k}_0$, and thus provides a distinctive measure of phase coherence surviving the ensemble average.

Recently, we have investigated localization effects in one- and two-dimensional magnetic model systems [24]. It is the purpose of this work to study CBS as a precursor for Anderson localization in chiral magnetic systems, where the presence of the DM interaction leads to a dispersion relation $\omega_{\mathbf{k}}$ with broken inversion symmetry, i.e., $\omega_{\mathbf{k}} = \omega_{2\mathbf{K}^{\mathrm{I}}-\mathbf{k}} \neq \omega_{-\mathbf{k}}$ ($\mathbf{K}^{\mathrm{I}}$ is determined by the DM vectors and is explained below). In such a system time-reversal symmetry of the spin waves is broken (since $\mathbf{k}$ and $-\mathbf{k}$ are not equivalent), and, in addition, $-\mathbf{k}_0$ is in general no longer a possible scattering vector under elastic scattering, and one should expect the CBS effect to be weakened, if not entirely suppressed. Surprisingly, we find by numerical investigations of an atomistic spin model that CBS survives in such a system with its peak position shifted to $2\mathbf{K}^{\mathrm{I}} - \mathbf{k}_0$. Remarkably, the height of the CBS peak is not affected at all, in contrast to other model systems [25] where a shifted coherence condition is generally accompanied by a loss of contrast [25]. We will show below that this observation can be explained within a diagrammatic Green's function approach.

II. SPIN-WAVE TRANSPORT IN A CHIRAL FERROMAGNET

We consider a classical atomistic spin model [26], where normalized magnetic moments $\mathbf{S}^l = \boldsymbol{\mu}^l/\mu_{\mathrm{S}}$, $l = 1,\ldots,N$, are placed on regular lattice sites $\mathbf{r}^l$, with $\boldsymbol{\mu}^l$ the magnetic moment of the atom at position $\mathbf{r}^l$ and μ_{S} its absolute value. In d dimensions each spin is coupled to its $2d$ nearest neighbors. The interaction of nearest neighbors $\mathbf{S}^n$ and $\mathbf{S}^m$ splits into the isotropic Heisenberg exchange interaction with exchange constant $J > 0$ and the DM interaction, quantified by the DM vectors $\mathbf{D}^{nm}$ and originating from spin-orbit coupling [27]. In addition we take into account an easy-axis anisotropy in the x direction with anisotropy constant $d_x > 0$. Finally, we also include an external, random magnetic field $\mathbf{B}(\mathbf{r}^l) = \mathbf{B}^l$ that models local disorder. The Hamiltonian of such a system is

$$H = -\frac{J}{2}\sum_{\langle n,m\rangle}\mathbf{S}^n\cdot\mathbf{S}^m - \frac{1}{2}\sum_{\langle n,m\rangle}\mathbf{D}^{nm}\cdot(\mathbf{S}^n\times\mathbf{S}^m)$$
$$- \sum_n d_x(S_x^n)^2 - \mu_{\mathrm{S}}\sum_n\mathbf{B}^n\cdot\mathbf{S}^n. \tag{1}$$

The spin dynamics in the limit of vanishing damping is governed by the Landau-Lifshitz equation

$$\frac{\partial \mathbf{S}^l}{\partial t} = -\frac{\gamma}{\mu_{\mathrm{S}}} \mathbf{S}^l \times \mathbf{H}^l, \qquad \mathbf{H}^l = -\frac{\partial H}{\partial \mathbf{S}^l}, \qquad (2)$$

describing the precession of each spin $\mathbf{S}^l$ in its effective magnetic field $\mathbf{H}^l$, where γ is the gyromagnetic ratio. It is natural to use $t_J = \mu_{\mathrm{S}}/\gamma J$ and $B_J = J/\mu_{\mathrm{S}}$ as units for time and magnetic field, respectively.

In the case of weak DM interaction, $|\mathbf{D}^{nm}| < 0.1J$, the ground state of the clean system ($\mathbf{B}^l = 0$) is a ferromagnet parallel to the x axis. Collective excitations of this ferromagnetic ground state, called magnons or spin waves, can be described by a complex spin-wave amplitude $\mathcal{S}^l = S_y^l - i S_z^l$ in real space. In the context of this work, it is more advantageous to describe spin waves via their momentum-space amplitude $\mathcal{S}_{\mathbf{k}} = \frac{1}{\sqrt{N}} \sum_n e^{-i \mathbf{k} \cdot \mathbf{r}^n} \mathcal{S}^n$. The dispersion of these spin waves in the linearized limit of small deviations from the clean ground state reads [13]

$$\omega_{\mathbf{k}} = \frac{1}{t_J} \left\{ \frac{d_x}{J} + 2 \sum_{p=1}^{d} \left[1 - \cos(\mathbf{k} \cdot \mathbf{a}^p) + \frac{D_x^p}{J} \sin(\mathbf{k} \cdot \mathbf{a}^p) \right] \right\}. \tag{3}$$

The sum runs over the d lattice vectors $\mathbf{a}^p$, and $\mathbf{D}^p$ denotes the DM vector $\mathbf{D}^{nm}$ between two spins $\mathbf{S}^n$ and $\mathbf{S}^m$ that are separated by $\mathbf{a}^p = \mathbf{r}^m - \mathbf{r}^n$. Because the ground state is aligned with the easy x axis, the dispersion only depends on the x component of the DM vectors. Importantly, the DM interaction breaks the inversion symmetry of the dispersion, $\omega_{\mathbf{k}} \neq \omega_{-\mathbf{k}}$. The sine term in the dispersion shifts the lines of constant frequency, resulting in a dispersion

$$\omega_{\mathbf{k}} = \omega_{2\mathbf{K}^{\mathrm{I}} - \mathbf{k}} \tag{4}$$

that is instead symmetric with respect to a shifted center of inversion $\mathbf{K}^{\mathrm{I}} \neq 0$ determined by

$$\mathbf{K}^{\mathrm{I}} \cdot \mathbf{a}^p = -\arctan\left(\frac{D_x^p}{J}\right), \qquad p = 1, \ldots, d. \tag{5}$$

Even in a weakly disordered magnetic material, plane waves are no longer eigenmodes and will be scattered elastically by static, quenched disorder into other accessible modes. In an inversion-symmetric setting, the CBS signal of a plane wave launched with wave vector $\mathbf{k}_0$ is found at $-\mathbf{k}_0$ [23]. In the case of a noninversion symmetric dispersion the initial wave cannot be scattered into the $-\mathbf{k}_0$ state, leading to the question whether CBS can survive in a chiral magnet at all.

III. NUMERICAL INVESTIGATIONS OF CBS

As a model for thin magnetic films we choose $d = 2$ and a square lattice with lattice constant $a = |\mathbf{a}^p|$, and perform numerical simulations of spin waves by integrating Eq. (2) using the classical Runge-Kutta method. The initial condition is a quasimonochromatic wave packet,

$$\mathcal{S}^l(t=0) = A \exp\left[i \mathbf{k}_0 \cdot \mathbf{r}^l - (\mathbf{r}^l - \mathbf{r}_0)^2 / 2\sigma_0^2\right], \tag{6}$$

with amplitude A and width σ_0 around the initial position $\mathbf{r}_0$. Throughout the paper we use $A = 0.01$, $\sigma_0 = 150a$ together

with the initial wave vector $\mathbf{k}_0 = (0.24, -0.48)\pi/a$, except where noted otherwise.

For concreteness, we consider disorder induced by a longitudinal field $\mathbf{B}^j = (B, 0, 0)$ that tries to pin the ferromagnetic orientation at randomly chosen lattice sites $\mathbf{r}^j$, with $\mathbf{B}^l = 0$ elsewhere. The defect sites are static, uncorrelated, and uniformly distributed with density ϱ. In the following, all simulations use $\varrho = 0.1$ and $B = 5B_J$, followed by an ensemble average $\langle \cdots \rangle$ over 500 defect configurations. This defect model has the advantage of acting on magnons as a disordered potential in the same manner as a space-dependent, disordered potential in the Schrödinger equation does; it is simple, its effects are well controllable, and requires less computational effort for the numerics than other models. However, our results in this work are not restricted to the aforementioned defect model, which we verified by using alternative models and obtaining the same results (except for different time scales as the scattering time). An example for these is to locally reduce the magnetic moment at randomly chosen lattice sites, which models impurity atoms in the magnet, and is closer to an experimental realization than the random-field model.

In a first step we choose $D_x^p = -0.08J$ and $D_y^p = D_z^p = 0$. Following the time evolution, we observe that the average spin-wave intensity in momentum space, $I_{\mathbf{k}} = \langle |\mathcal{S}_{\mathbf{k}}|^2 \rangle$, that is initially concentrated at $\mathbf{k}_0$ redistributes over the other accessible modes $\mathbf{k}$ on the energy shell $\omega_{\mathbf{k}} = \omega_{\mathbf{k}_0}$, slightly broadened by disorder. Phase-incoherent diffusion alone would result in a homogeneous distribution, reached on a rather fast time scale given by the transport time [28]. Distinctive features above this incoherent background are signatures of phase-coherent processes [24,29]. After a few transport times, the spin-wave intensity in k space can thus be written $I_{\mathbf{k}}(t) = I_{\mathbf{k}}^{\mathrm{ic}} + I_{\mathbf{k}}^{\mathrm{c}}(t)$, where $I_{\mathbf{k}}^{\mathrm{ic}}$ denotes the incoherent, stationary contribution and $I_{\mathbf{k}}^{\mathrm{c}}(t)$ is the part that originates from coherent processes and evolves on longer time scales.

Figure 1(a) shows $I_{\mathbf{k}}(t)$ at a time $t = 20t_J$. The incoherent background $I_{\mathbf{k}}^{\mathrm{ic}}$ maps out the disorder-broadened energy shell. A clear backscattering peak is observable roughly opposite the initial wave vector $\mathbf{k}_0$. Interestingly, the CBS peak position differs from the exact backscattering direction $-\mathbf{k}_0$ that is well known from the inversion-symmetric setting [23]. In the present setting, the backscattering peak appears at the conjugate of $\mathbf{k}_0$ with respect to the center of inversion $\mathbf{K}^{\mathrm{I}}$, namely, at $\mathbf{k}_{\mathrm{CBS}} = 2\mathbf{K}^{\mathrm{I}} - \mathbf{k}_0$. This is remarkable since the backscattering wave vector is not antiparallel to the initial wave vector anymore, but clearly compatible with the symmetry, Eq. (4), of the dispersion relation.

While the DM interaction is apparently compatible with CBS at early times, although with a shifted peak position, it could very well induce a slight dephasing on longer times scales and therefore result in a faster decay of the CBS peak contrast. We investigate this question by recording the time evolution of the CBS contrast $\mathcal{C}(t) = I_{\mathbf{k}_{\mathrm{CBS}}}^{\mathrm{c}}(t)/I_{\mathbf{k}_{\mathrm{CBS}}}^{\mathrm{ic}}$ and comparing the cases with and without DM interaction under otherwise identical conditions. Even without any additional dephasing processes, the CBS contrast decreases over time because the diffusive CBS interference kernel, whose k-space resolution increases over time, is convolved by the finite-width wave packet, Eq. (6), leading to an expected decay as $\mathcal{C}(t) = (1 + Dt/2\sigma_0^2)^{-1}$, where D is the spin-wave diffusion constant
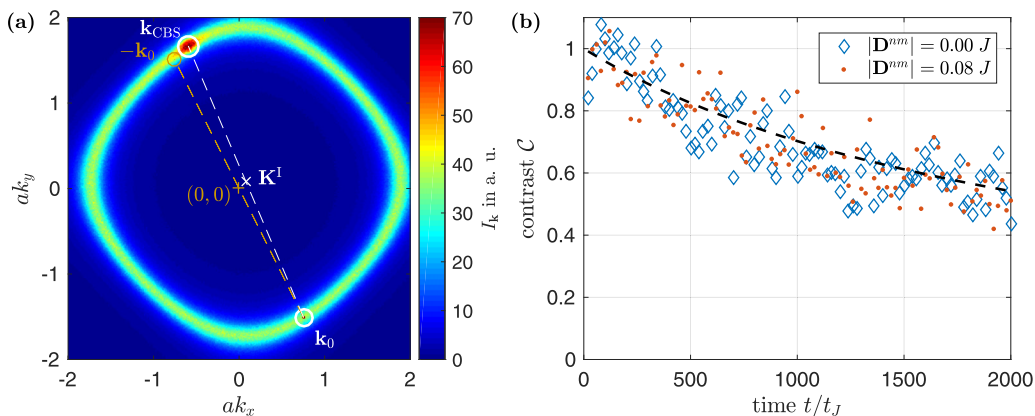
FIG. 1. CBS of spin waves in chiral magnets with DM interaction. (a) Ensemble-averaged spin-wave intensity in k space, $I_{\mathbf{k}} = \langle |\mathcal{S}_{\mathbf{k}}|^2 \rangle$ at time $t = 20t_J$. The initial wave packet [Eq. (6)] is centered at $\mathbf{k}_0$. A CBS peak rises at $\mathbf{k}_{\mathrm{CBS}} \neq -\mathbf{k}_0$ over the incoherent background. Both the center of the Brillouin zone $\Gamma = (0,0)$ and the center of inversion $\mathbf{K}^{\mathrm{I}}$ are plotted. The CBS peak position is the conjugate of $\mathbf{k}_0$ with respect to $\mathbf{K}^{\mathrm{I}}$, namely, $\mathbf{k}_{\mathrm{CBS}} - \mathbf{K}^{\mathrm{I}} = \mathbf{K}^{\mathrm{I}} - \mathbf{k}_0$. (b) Time evolution of the CBS contrast with and without DM interaction. The dashed curve is the expected decay $\mathcal{C}(t) = (1 + Dt/2\sigma_0^2)^{-1}$ with spin-wave diffusion constant $D \approx 19\,a^2/t_J$ extracted from the real-space diffusive spread of the wave packet. Within the noise of the data, there is no observable difference between the cases with and without DM interaction.

[24,29]. The numerical results, shown in Fig. 1(b), indicate that within the noise of the data the DM interaction does not accelerate this decay significantly and thus does not act as an additional source of dephasing.

According to linear spin-wave theory within the present geometry only the x component of the DM vectors influences the dispersion relation, Eq. (4). We have also confirmed this prediction numerically by simulating a system with $D_y^p = D_z^p \neq 0$ and $D_x^p = 0$. The result is then the same as in the case with $\mathbf{D}^p = 0$. Because linear spin-wave theory can only be applied for small amplitudes, we have also tested a larger amplitude, $A = 0.2$, and compared again the two cases, $\mathbf{D}^p = 0$ and $D_x^p = -0.08\,J$. The decay of the CBS contrast is in both cases much faster than in the linear regime, as a consequence of the nonlinearities in the equations of motion that arise for larger amplitudes [24]. Still, however, the system with DM interaction shows a decay of the CBS peak just as fast as the system without DM interaction. We infer from the numerical evidence that the DM interaction does not lower the CBS contrast nor does it lead to faster dephasing, it simply shifts the backscattering wave vector to a different position.

IV. DIAGRAMMATIC DESCRIPTION OF CBS IN THE LINEAR REGIME

Our numerical findings in the linear regime can be readily understood via a diagrammatic Green's function approach. The argument relies, besides the symmetry Eq. (4) of the dispersion, on the fact that a pointlike pinning field results in a completely isotropic scattering intensity, noted $U_{\mathbf{k}\mathbf{k}'} = U_0$. As a consequence, the ensemble-averaged, single-magnon Green's function takes the form $G_{\mathbf{k}}(\omega) = [\omega - \omega_{\mathbf{k}} - \Sigma(\omega)]^{-1}$, diagrammatically represented by Fig. 2(a), with a self-energy $\Sigma(\omega) = U_0 \sum_{\mathbf{q}} G_{\mathbf{q}}(\omega) + \cdots$ that has no momentum dependence on its own. Thus, the Green's function inherits the generalized inversion symmetry (4) from the dispersion, namely,

$$G_{\mathbf{k}}(\omega) = G_{2\mathbf{K}^{\mathrm{I}} - \mathbf{k}}(\omega). \tag{7}$$

We proceed to show that the CBS peak height at $\mathbf{k}_{\mathrm{CBS}} = 2\mathbf{K}^{\mathrm{I}} - \mathbf{k}_0$ equals the incoherent background contribution. The stationary background $\mathbf{k}$-space distribution is described by an intensity propagation kernel that can be represented by the ladder diagram of Fig. 2(b), depicting a retarded and an advanced amplitude copropagating along the same impurities. Its nth − order term describes the scattering by n impurities, connected by $n - 1$ intensity Green's functions at intermediate momenta $\mathbf{q}_j$:

$$L_n(\mathbf{k}_0, \mathbf{k}, \omega) = U_0^n \prod_{j=1}^{n-1} \sum_{\mathbf{q}_j} G_{\mathbf{q}_j}(\omega) G_{\mathbf{q}_j}^*(\omega). \tag{8}$$

The corresponding CBS contribution arises from the interference of two amplitudes counterpropagating along the same impurities, but in opposite order, and can be represented by the maximally crossed diagram of Fig. 2(c). Its nth − order term reads, by virtue of momentum conservation at each average impurity scattering event,

$$C_n(\mathbf{k}_0, \mathbf{k}, \omega) = U_0^n \prod_{j=1}^{n-1} \sum_{\mathbf{q}_j} G_{\mathbf{q}_j}(\omega) G_{\mathbf{k}_0 + \mathbf{k} - \mathbf{q}_j}^*(\omega). \tag{9}$$
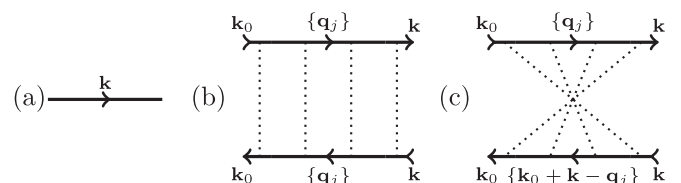

FIG. 2. (a) Diagrammatic representation for the ensemble-averaged Green's function, Eq. (7). (b) Incoherent background intensity kernel, a sum of ladder diagrams [Eq. (8)]. (c) CBS contribution given by the sum of maximally crossed diagrams [Eq. (9)]. Upon choosing $\mathbf{k} + \mathbf{k}_0 = 2\mathbf{K}^{\mathrm{I}}$, this contribution equals the background of (b) and thus yields perfect interference contrast at the shifted position $\mathbf{k}_{\mathrm{CBS}} = 2\mathbf{K}^{\mathrm{I}} - \mathbf{k}_0$.

At final momentum $\mathbf{k} = 2\mathbf{K}^{\mathrm{I}} - \mathbf{k}_0$, the generalized inversion symmetry (7) then guarantees that the crossed contribution (9) equals the background contribution (8), order by order for all $n \geqslant 2$ beyond the single scattering term that is irrelevant at longer times. In the end, perfect contrast is achieved for the entire CBS signal at the shifted peak position $\mathbf{k}_{\mathrm{CBS}} = 2\mathbf{K}^{\mathrm{I}} - \mathbf{k}_0$.

V. DISCUSSION AND SUMMARY

A shift of the backscattering peak is known from transport of light in turbid media in the presence of magneto-optical Faraday rotation [25]. However, the situation in Faraday experiments differs from the magnetic system studied here in that the shift of the CBS peak is always accompanied by a loss of contrast. This dephasing is caused by a random shift of the transverse photon polarization at every scattering event, eventually breaking the reciprocity symmetry that would otherwise preserve the CBS contrast. In our system reciprocity remains intact since the spin-wave polarization is not constrained by transversality and remains unchanged under scattering by scalar impurities.

The DM interaction originates from spin-orbit coupling of localized or itinerant electrons [10,30], which calls for a comparison to electronic transport where spin-orbit coupling has a great impact on weak localization [31]. For electrons strong spin-orbit coupling leads to so-called weak antilocalization [32], where the amplitudes interfering for CBS collect a phase difference of 2π. Because electrons are spin-$\frac{1}{2}$ particles, this phase difference implies a sign change that results in destructive interference such that the scattered intensity is lower in the backscattering direction. The ferromagnetic magnons considered in this work do not own a polarizationlike degree of freedom as electrons own a spin, such that they do not collect such a 2π phase difference. In other magnetic materials the situation could be different; for example, antiferromagnets have two magnon branches with opposite polarizations, but obviously even in such a case a 2π phase difference does not affect CBS since for bosonic excitations this phase difference implies constructive interference, so that no antilocalization would be expected from the start.

In an experimental setup, magnetic damping effects play an important role, which we neglected so far. However, Gilbert damping affects all modes uniformly, such that the overall intensity is lowered, but the contrast is preserved. This was already shown in [24] for ferromagnetic spin waves without DM interaction and still holds true here with DM interaction, as we have confirmed in additional simulations, which are not shown here.

In conclusion we have investigated coherent backscattering in a chiral magnetic system with point defects where the dispersion exhibits a broken inversion symmetry that shifts the CBS peak but preserves its contrast. Our numerical findings can be understood in terms of a diagrammatic approach using the shifted symmetry of the dispersion, $\omega_{\mathbf{k}} = \omega_{2\mathbf{K}^{\mathrm{I}} - \mathbf{k}}$. The main message is that DM interaction shifts the CBS peak away from the normal $-\mathbf{k}_0$ direction without altering the contrast or the decay time. It is surprising to find weak localization in a system with broken time-reversal symmetry. However, it is well known from optics that time-reversal symmetry is a sufficient condition for weak localization and not a necessary one. Instead, weak localization requires that the reciprocity theorem holds [33], and in the case of the spin-wave system studied here this reciprocity is given by the equivalence of $\mathbf{k}$ and $2\mathbf{K}^{\mathrm{I}} - \mathbf{k}$, such that the system still shows weak localization.

Since the shift of the CBS peak is directly proportional to the DM vectors by virtue of Eq. (5), measuring the CBS position provides a way to determine the strength as well as the sign of the DM interaction. For this, a few alternative methods are available, like Brillouin light scattering [34], spin polarized scanning tunneling microscopy [35], propagating spin-wave spectroscopy [36], and domain-wall motion [37,38]. However, especially for amorphous materials like CoFeB, different methods may lead to different results [39] and a clear determination of the strength and sign of the DM interaction is still a matter of research. The CBS effect offers yet another method that may help to clarify this issue.

[1] V. V. Kruglyak, S. O. Demokritov, and D. Grundler, Magnonics, J. Phys. D: Appl. Phys. **43**, 264001 (2010).

[2] *Magnonics. From Fundamentals to Applications*, edited by S. O. Demokritov and A. N. Slavin (Springer, Berlin/Heidelberg, 2013).

[3] K. Uchida, J. Xiao, H. Adachi, J. Ohe, S. Takahashi, J. Ieda, T. Ota, Y. Kajiwara, H. Umezawa, H. Kawai, G. E. W. Bauer, S. Maekawa, and E. Saitoh, Spin Seebeck insulator, Nat. Mater. **9**, 894 (2010).

[4] S. O. Demokritov, V. E. Demidov, O. Dzyapko, G. A. Melkov, A. A. Serga, B. Hillebrands, and A. N. Slavin, Bose-Einstein condensation of quasi-equilibrium magnons at room temperature under pumping, Nature (London) **443**, 430 (2006).

[5] D. A. Bozhko, A. A. Serga, P. Clausen, V. I. Vasyuchka, F. Heussner, G. A. Melkov, A. Pomyalov, V. S. L'vov, and B. Hillebrands, Supercurrent in a room-temperature Bose-Einstein magnon condensate, Nat. Phys. **12**, 1057 (2016).

[6] L. Zhang, J. Ren, J.-S. Wang, and B. Li, Topological magnon insulator in insulating ferromagnet, Phys. Rev. B **87**, 144101 (2013).

[7] A. A. Serga, A. V. Chumak, and B. Hillebrands, YIG magnonics, J. Phys. D: Appl. Phys. **43**, 264002 (2010).

[8] G. E. W. Bauer, E. Saitoh, and B. J. van Wees, Spin caloritronics, Nat. Mater. **11**, 391 (2012).

[9] I. Dzyaloshinsky, A thermodynamic theory of "weak" ferromagnetism of antiferromagnetics, J. Phys. Chem. Solids **4**, 241 (1958).

[10] T. Moriya, New Mechanism of Anisotropic Superexchange Interaction, Phys. Rev. Lett. **4**, 228 (1960).

[11] Y. Togawa, T. Koyama, K. Takayanagi, S. Mori, Y. Kousaka, J. Akimitsu, S. Nishihara, K. Inoue, A. S. Ovchinnikov, and J. Kishine, Chiral Magnetic Soliton Lattice on a Chiral Helimagnet, Phys. Rev. Lett. **108**, 107202 (2012).

[12] U. K. Rößler, A. N. Bogdanov, and C. Pfleiderer, Spontaneous skyrmion ground states in magnetic metals, Nature (London) **442**, 797 (2006).

[13] L. Udvardi and L. Szunyogh, Chiral Asymmetry of the Spin-Wave Spectra in Ultrathin Magnetic Films, Phys. Rev. Lett. **102**, 207204 (2009).

[14] K. Zakeri, Y. Zhang, J. Prokop, T.-H. Chuang, N. Sakr, W. X. Tang, and J. Kirschner, Asymmetric Spin-Wave Dispersion on Fe(110): Direct Evidence of the Dzyaloshinskii-Moriya Interaction, Phys. Rev. Lett. **104**, 137203 (2010).

[15] J.-H. Moon, S.-M. Seo, K.-J. Lee, K.-W. Kim, J. Ryu, H.-W. Lee, R. D. McMichael, and M. D. Stiles, Spin-wave propagation in the presence of interfacial Dzyaloshinskii-Moriya interaction, Phys. Rev. B **88**, 184404 (2013).

[16] A. Manchon and S. Zhang, Theory of nonequilibrium intrinsic spin torque in a single nanomagnet, Phys. Rev. B **78**, 212405 (2008).

[17] A. Manchon and S. Zhang, Theory of spin torque due to spin-orbit coupling, Phys. Rev. B **79**, 094422 (2009).

[18] A. R. Mellnik, J. S. Lee, A. Richardella, J. L. Grab, P. J. Mintun, M. H. Fischer, A. Vaezi, A. Manchon, E.-A. Kim, N. Samarth, and D. C. Ralph, Spin-transfer torque generated by a topological insulator, Nature (London) **511**, 449 (2014).

[19] O. Gomonay, T. Jungwirth, and J. Sinova, High Antiferromagnetic Domain Wall Velocity Induced by Néel Spin-Orbit Torques, Phys. Rev. Lett. **117**, 017202 (2016).

[20] T. Shiino, S.-H. Oh, P. M. Haney, S.-W. Lee, G. Go, B.-G. Park, and K.-J. Lee, Antiferromagnetic Domain Wall Motion Driven by Spin-Orbit Torques, Phys. Rev. Lett. **117**, 087203 (2016).

[21] F. Hellman, A. Hoffmann, Y. Tserkovnyak, G. S. D. Beach, E. E. Fullerton, C. Leighton, A. H. MacDonald, D. C. Ralph, D. A. Arena, H. A. Dürr, P. Fischer, J. Grollier, J. P. Heremans, T. Jungwirth, A. V. Kimel, B. Koopmans, I. N. Krivorotov, S. J. May, A. K. Petford-Long, J. M. Rondinelli, N. Samarth, I. K. Schuller, A. N. Slavin, M. D. Stiles, O. Tchernyshyov, A. Thiaville, and B. L. Zink, Interface-induced phenomena in magnetism, Rev. Mod. Phys. **89**, 025006 (2017).

[22] P. W. Anderson, Absence of Diffusion in Certain Random Lattices, Phys. Rev. **109**, 1492 (1958).

[23] E. Akkermans and G. Montambaux, *Mesoscopic Physics of Electrons and Photons* (Cambridge University Press, Cambridge, UK, 2007).

[24] M. Evers, C. A. Müller, and U. Nowak, Spin-wave localization in disordered magnets, Phys. Rev. B **92**, 014411 (2015).

[25] R. Lenke and G. Maret, Magnetic field effects on coherent backscattering of light, Eur. Phys. J. B **17**, 171 (2000).

[26] U. Nowak, Classical Spin Models, in *Handbook of Magnetism and Advanced Magnetic Materials*, Vol. 2, edited by H. Kronmüller and S. Parkin (Wiley, New York, 2007).

[27] L. Udvardi, L. Szunyogh, K. Palotás, and P. Weinberger, First-principles relativistic study of spin waves in thin magnetic films, Phys. Rev. B **68**, 104436 (2003).

[28] T. Plisson, T. Bourdel, and C. A. Müller, Momentum isotropisation in random potentials, Eur. Phys. J.: Spec. Top. **217**, 79 (2013).

[29] N. Cherroret, T. Karpiuk, C. A. Müller, B. Grémaud, and C. Miniatura, Coherent backscattering of ultracold matter waves: Momentum space signatures, Phys. Rev. A **85**, 011604 (2012).

[30] A. Fert and P. M. Levy, Role of Anisotropic Exchange Interactions in Determining the Properties of Spin-Glasses, Phys. Rev. Lett. **44**, 1538 (1980).

[31] S. Hikami, A. I. Larkin, and Y. Nagaoka, Spin-orbit interaction and magnetoresistance in the two dimensional random system, Prog. Theor. Phys. **63**, 707 (1980).

[32] G. Bergmann, Physical interpretation of weak localization: A time-of-flight experiment with conduction electrons, Phys. Rev. B **28**, 2914 (1983).

[33] B. A. van Tiggelen and R. Maynard, Reciprocity and coherent backscattering of light, in *Wave Propagation in Complex Media*, edited by G. Papanicolaou (Springer, New York, 1998), pp. 247–271.

[34] K. Di, V. L. Zhang, H. S. Lim, S. C. Ng, M. H. Kuok, J. Yu, J. Yoon, X. Qiu, and H. Yang, Direct Observation of the Dzyaloshinskii-Moriya Interaction in a Pt/Co/Ni Film, Phys. Rev. Lett. **114**, 047201 (2015).

[35] M. Bode, M. Heide, K. von Bergmann, P. Ferriani, S. Heinze, G. Bihlmayer, A. Kubetzka, O. Pietzsch, S. Blügel, and R. Wiesendanger, Chiral magnetic order at surfaces driven by inversion asymmetry, Nature (London) **447**, 190 (2007).

[36] J. M. Lee, C. Jang, B.-C. Min, S.-W. Lee, K.-J. Lee, and J. Chang, All-electrical measurement of interfacial Dzyaloshinskii-Moriya interaction using collective spin-wave dynamics, Nano Lett. **16**, 62 (2016).

[37] S.-G. Je, D.-H. Kim, S.-C. Yoo, B.-C. Min, K.-J. Lee, and S.-B. Choe, Asymmetric magnetic domain-wall motion by the Dzyaloshinskii-Moriya interaction, Phys. Rev. B **88**, 214401 (2013).

[38] A. Hrabec, N. A. Porter, A. Wells, M. J. Benitez, G. Burnell, S. McVitie, D. McGrouther, T. A. Moore, and C. H. Marrows, Measuring and tailoring the Dzyaloshinskii-Moriya interaction in perpendicularly magnetized thin films, Phys. Rev. B **90**, 020402 (2014).

[39] R. Soucaille, M. Belmeguenai, J. Torrejon, J.-V. Kim, T. Devolder, Y. Roussigné, S.-M. Chérif, A. A. Stashkevich, M. Hayashi, and J.-P. Adam, Probing the Dzyaloshinskii-Moriya interaction in CoFeB ultrathin films using domain wall creep and Brillouin light spectroscopy, Phys. Rev. B **94**, 104431 (2016).